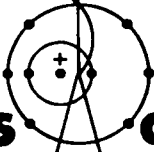


LA-4918

C. 3

CIC-14 REPORT COLLECTION  
REPRODUCTION  
COPY

Evaluated Neutron-Induced  
Gamma-Ray Production Cross Sections  
for  $^{235}\text{U}$  and  $^{238}\text{U}$



**los alamos**  
**scientific laboratory**

of the University of California

LOS ALAMOS, NEW MEXICO 87544



This report was prepared as an account of work sponsored by the United States Government. Neither the United States nor the United States Atomic Energy Commission, nor any of their employees, nor any of their contractors, subcontractors, or their employees, makes any warranty, express or implied, or assumes any legal liability or responsibility for the accuracy, completeness or usefulness of any information, apparatus, product or process disclosed, or represents that its use would not infringe privately owned rights.

Printed in the United States of America. Available from  
National Technical Information Service  
U. S. Department of Commerce  
5285 Port Royal Road  
Springfield, Virginia 22151  
Price: Printed Copy \$3.00; Microfiche \$0.95

LA-4918

UC-34

ISSUED: July 1972

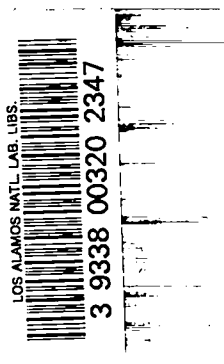


**los alamos**  
**scientific laboratory**  
of the University of California  
LOS ALAMOS, NEW MEXICO 87544

# Evaluated Neutron-Induced Gamma-Ray Production Cross Sections for $^{235}\text{U}$ and $^{238}\text{U}$

by

L. Stewart  
R. E. Hunter\*



\*Mr. Hunter was a consultant to the Los Alamos  
Scientific Laboratory at the time this report was written.



EVALUATED NEUTRON-INDUCED GAMMA-RAY PRODUCTION CROSS SECTIONS  
FOR  $^{235}\text{U}$  AND  $^{238}\text{U}$

by

L. Stewart and R. E. Hunter

ABSTRACT

The gamma-ray production cross sections produced by neutron interactions from  $10^{-5}$  eV to 20 MeV have been evaluated for  $^{235}\text{U}$  and  $^{238}\text{U}$ . The data were prepared for input into the ENDF/B format. Below 1 MeV, the "prompt" fission and radiative-capture spectra are included along with the gammas from inelastic scattering. Above 1 MeV, the total gamma-ray production cross sections from all nonelastic processes are input as a single reaction since the experimental measurements did not discriminate between the individual reaction channels. At all energies, all gamma rays are assumed to be emitted isotropically.

I. INTRODUCTION

Gamma-ray production cross sections for various nuclides are required as input data for radiation shielding, heating, and gamma-ray-transport calculations. The experimental data on  $^{235}\text{U}$  and  $^{238}\text{U}$  are evaluated and combined with calculations to produce a set of recommended cross sections. This effort was to some extent the outgrowth of a more extensive effort on  $^{239}\text{Pu}$  and  $^{240}\text{Pu}$ , the results of which are discussed in Ref. 1. The reader is referred to that report for the details of certain calculations that are only summarized here. The authors will remark only that experimental data are far from extensive and that considerable reliance was necessarily placed on calculations and on extrapolation of data from other nuclides.

Experimental data exist in three forms: (1) the gamma-ray spectrum associated with fission

events (for a given time after fission) has been measured<sup>2,3</sup> for thermal neutrons incident on  $^{235}\text{U}$ ; (2) the radiative-capture spectrum has been measured<sup>4,5</sup> for  $^{238}\text{U}$  at a number of incident neutron energies between thermal and 101.9 keV; and (3) the total gamma-ray production cross sections have been measured<sup>6,7</sup> for  $^{235}\text{U}$  and/or  $^{238}\text{U}$  at several incident-neutron energies between 1.09 and 14.8 MeV. These measurements are presented as absolute cross sections per MeV for  $E_\gamma$  above 250 or 500 keV for gamma-ray-energy intervals of 250 or 500 keV. The extrapolation of these data to  $E_\gamma = 0$  to obtain integrated total gamma-ray production cross sections adds significantly to the uncertainty in the evaluated results.

The thermal-capture spectrum for  $^{235}\text{U}$  has not been observed although Journey and Sheline<sup>8</sup> measured the line spectra for  $E_\gamma > 3.3$  MeV at thermal and

provided these data in terms of cross sections. These discrete lines could sometimes be ascribed to the fission process and sometimes to radiative capture, but few of the gamma rays were uniquely assigned. It is reasonable to assume that the discrete lines above 3.3 MeV would account for a small portion of the total gamma-ray production cross section; therefore, these data provide only a check on the total integral values.

## II. URANIUM-235

As discussed in the Introduction, data on  $^{235}\text{U}$  are sparse. In particular, no data exist on the angular distributions of the gamma rays produced from particular neutron reactions on  $^{235}\text{U}$ , although Nellis and Morgan<sup>6</sup> found the total gamma-ray production cross sections to be isotropic within  $\pm 10\%$  at incident neutron energies of 1.09, 4.0, and 14.8 MeV. In the absence of data to the contrary, it is assumed that all gamma-ray processes are isotropic.

Since the absolute cross sections at some energies must be obtained by using multiplicities, whereas measurements at other energies are reported in barns/MeV, it seemed desirable to separate the neutron-energy range for discussion as follows:

- (1) The thermal region up to the onset of inelastic scattering;
- (2) The region from the inelastic threshold up to 1.09 MeV;
- (3) 1.09 to 20 MeV.

### A. $10^{-5}$ eV to 13 keV

#### 1. Radiative Capture

In the absence of experimental data, the radiative-capture gamma-ray spectrum was taken to be the same as that for  $^{239}\text{Pu}$  in Ref. 1 which, in turn, was based on measurements by Orphan et al.<sup>9</sup>

on Hf. The probability distribution, normalized to one photon per capture, is shown in Fig. 1.

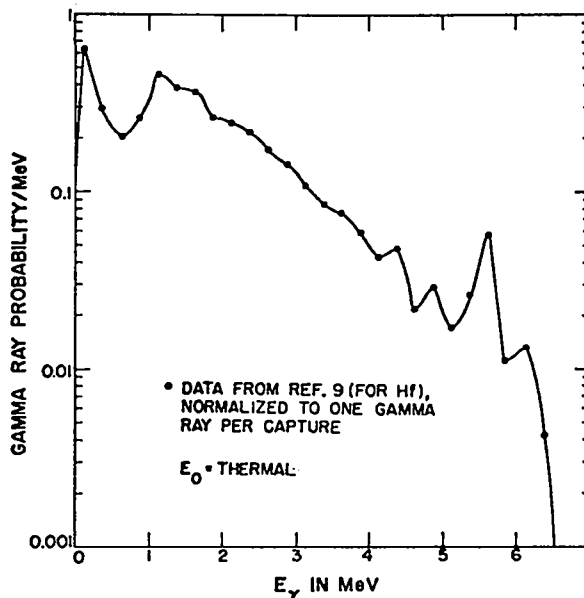


Fig. 1. Probability for production of photons as a function of  $E_\gamma$  due to capture by  $^{235}\text{U}$  (normalized to one gamma ray per capture) for thermal neutrons. Values are obtained from data on hafnium<sup>9</sup> adjusted to the binding energy of  $^{235}\text{U}$ .

#### 2. Fission

Measurements have been reported recently by Verbinski and Sund<sup>2</sup> and by Peelle and Maienschein<sup>3</sup> on the fission gamma-ray spectrum from  $^{235}\text{U}$  for thermal neutrons. Earlier measurements given by Maienschein et al.<sup>10</sup> and Rau,<sup>11</sup> were not used in this evaluation. (Note, however, that the earlier data of Ref. 10 form the basis for the reanalysis given in Ref. 3.)

Since Verbinski and Sund<sup>2</sup> provided better discrimination against neutron events in their measurements, it was decided to base this evaluation primarily on their data. Hence, after making a crude extrapolation of a smooth curve drawn through their data, a value of 6.7 MeV/fission was chosen for the total gamma-ray energy, corresponding to

gammas emitted within about 100 nsec after fission. Again, it should be noted that about 8 MeV/fission is carried off by photons following  $\beta$ -decay of the fission products; the emission times for these photons are long compared to the times associated here with "prompt" gammas.

The measurements on the fission gamma-ray spectrum, in absolute numbers of gamma rays per MeV per fission, are shown in Fig. 2. This spectrum, normalized to one photon per fission, is assumed to apply up to 1.09 MeV (that is, the spectrum is assumed to be independent of incident neutron energy).

### 3. Summary

To obtain the gamma-ray production cross sections, the probability distributions for fission and capture must be multiplied by the appropriate neutron cross sections and the correct multiplicities at each neutron energy.

#### B. 13 keV to 1.09 MeV

##### 1. Radiative Capture

At the lowest energy, the thermal capture spectrum is used. At 1.09 MeV, the capture spectrum has been modified somewhat arbitrarily to give the energy deposit required ( $E_0 + E_b$ , or 7.52 MeV); linear extrapolation is recommended between 13 keV and 1.09 MeV. The normalized spectrum is shown in Fig. 3.

##### 2. Fission

A review by James<sup>12</sup> shows that the total gamma-ray energy released per fission does not change significantly with incident neutron energy; therefore the gamma-ray energy distribution and multiplicity obtained from thermal measurements were used up to  $E_0 = 1.09$  MeV. This assumption is not quite valid, however, since the increase in  $\bar{\nu}$  with increasing neutron energy does not completely account

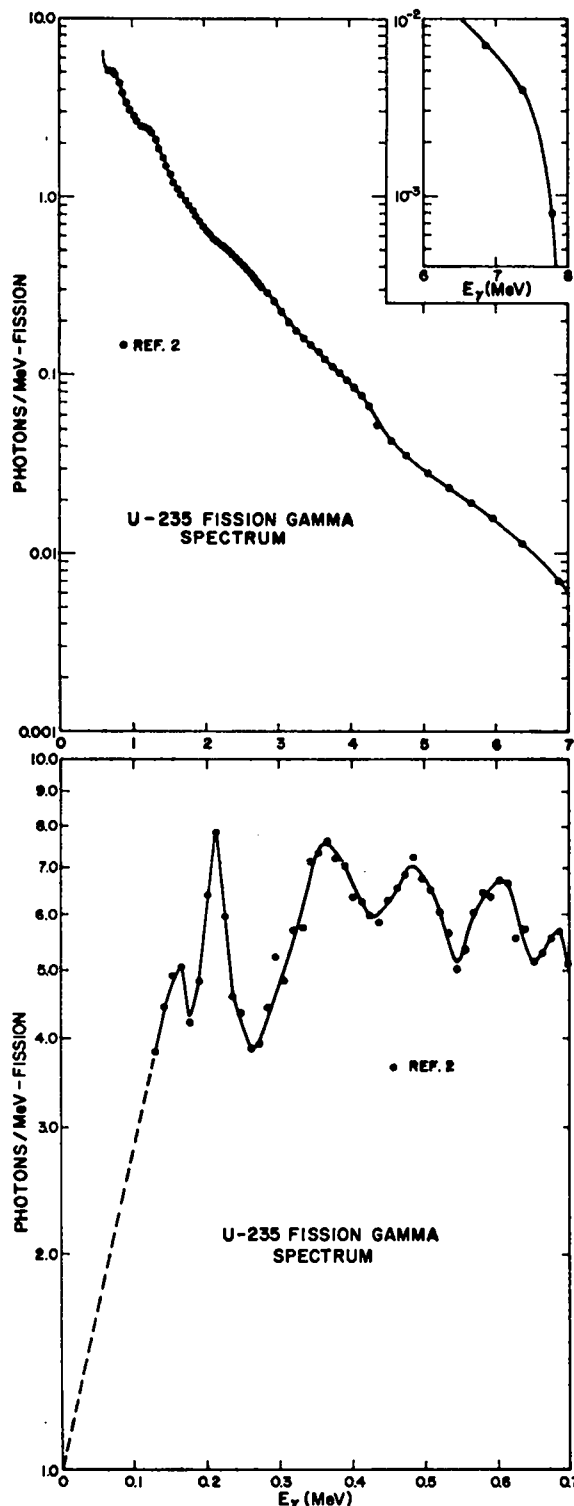


Fig. 2. The number of gamma rays per MeV per fission for  $^{235}\text{U}$  (top) and  $^{238}\text{U}$  (bottom) for thermal neutrons as a function of  $E_\gamma$ .

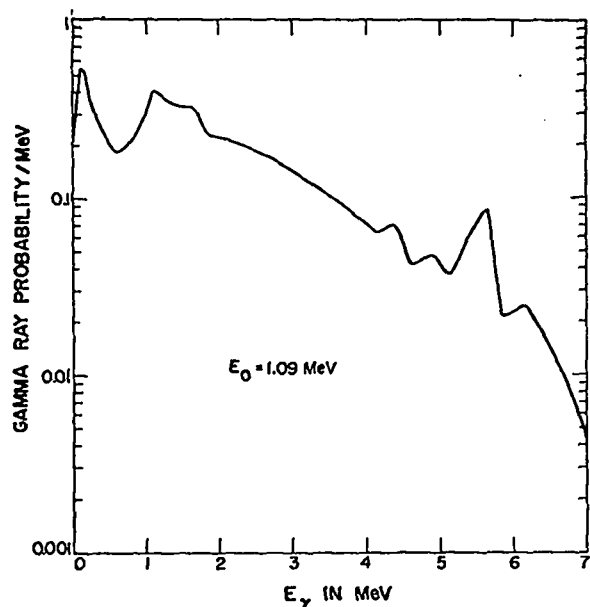


Fig. 3. Probability for production of photons as a function of  $E_\gamma$ , due to capture by  $^{235}\text{U}$  (normalized to one gamma ray per capture) for 1.09 MeV incident neutron energy.

for the increased energy available to the total system. In the absence of data to the contrary, however, the fission gamma-ray spectrum has been assumed to be energy-independent up to 1.09 MeV.

### 3. Inelastic Scattering

Gamma-ray spectra produced by inelastic scattering were calculated using the neutron cross sections for the various inelastic levels and the continuum given in the evaluation of Berlijn et al.<sup>13</sup> and the branching ratios given by Lederer et al.<sup>14</sup> (the 80-eV, 26.1-min isomeric state was ignored). The gamma-ray spectra were calculated at a number of points between the inelastic threshold at 13.055 keV and 1.09 MeV. From these, gamma-ray multiplicities were calculated using the total inelastic cross sections given by Berlijn et al.

Gamma-ray production cross sections can then be obtained by multiplying these multiplicities by the neutron inelastic-scattering cross sections. At incident neutron energies between these points,

gamma-ray production cross sections should be obtained by linear interpolation on the multiplicities.

### C. 1.09 to 20 MeV

Nellis and Morgan<sup>6</sup> and Drake<sup>7</sup> have reported measurements of the total gamma-ray spectra from 1.09 to 14.8 MeV. Uncertainties in these data are quoted as  $\pm 20$  and  $\pm 10\%$ , respectively, so that a corresponding uncertainty is reflected in drawing smooth curves to represent the gamma-ray spectra. As noted in the Introduction, the extrapolation to  $E_\gamma = 0$  presents rather serious problems and additional uncertainties. For example, this extrapolation (for  $0 \leq E \leq 0.5$  MeV) alone accounts for 33 to 70% for  $^{238}\text{U}$  (see Tables VII and XIII at the end of this report).

The uncertainty in the absolute magnitude of the spectra is constrained by the energy conservation relation:

$$\int_0^\infty E_\gamma \sigma_{\text{prod}}(E_\gamma) dE_\gamma = E_{\gamma f} \sigma_{n,f} + (E_0 - \bar{E}_n) \sigma_{n,1} + (E_0 + E_b) \sigma_{n,\gamma} + (E_0 + Q_{2n} - 2\bar{E}_{2n}) \sigma_{n,2n} + (E_0 + Q_{3n} - 3\bar{E}_{3n}) \sigma_{n,3n}, \quad (1)$$

where  $\bar{E}_{\gamma f}$  is the average total gamma-ray energy per fission event, and  $\bar{E}_n$ ,  $\bar{E}_{2n}$ , and  $\bar{E}_{3n}$  are the average energies of the neutrons from inelastic, (n,2n) and (n,3n) processes.

The absolute magnitudes of the gamma-ray distributions were checked against Eq. (1). The differences were always within the quoted experimental errors for the gamma-ray data and the neutron cross sections except for the spectrum at 7.5-MeV incident neutron energy.

At 7.5 MeV, Drake<sup>7</sup> reports  $17.0 \pm 1.5$  MeV-barns for the integral:

$$4\pi \int_0^{E_{\max}} E_{\gamma} \sigma(E_0, \theta_{\gamma}, E_{\gamma}) \Delta E_{\gamma} .$$

Integrating his experimental points directly by assuming that the  $E_{\gamma 1}$  represent the midpoints of the energy intervals gives only 14 MeV-barns for  $E_{\gamma} > 250$  keV. Drake's extrapolation below 250 keV would be consistent with a cross section of 8 barns/sr  $\text{MeV}^{-1}$ . In the next energy interval ( $E_{\gamma} = 250$  to 500 keV), Drake reports a measurement six times lower than this extrapolated value.

In an attempt to uncover the source of this discrepancy, the above integral was again performed while assuming that the  $E_{\gamma 1}$  represent the maximum energy allowed within the interval  $\Delta E_{\gamma}$ , but this exercise accounted for only 1/3 of the difference. It is concluded that Drake's integral value is inconsistent with his pointwise data at 7.5 MeV. A curve was drawn through Drake's data and then adjusted upward to agree more closely with his quoted integral value; the resultant curve lies well within the range of Eq. (1).

The gamma-ray cross sections and spectra were extended to  $E_0 = 20$  MeV by extrapolating the data at each gamma-ray energy as a function of incident neutron energy. Both the experimental data and evaluated curves for the various incident neutron energies are shown in Fig. 4; the ordinates are in barns/MeV and the abscissas are the gamma-ray energy in MeV. The total gamma-ray production cross sections given here correspond to all nonelastic processes.

### III. URANIUM-238

#### A. $10^{-5}$ eV to 45 keV

Only radiative capture produces gamma rays in the exit channel in this energy range. John and Orphan<sup>4</sup> measured the radiative-capture spectrum for 15 neutron energy intervals between 5.6 eV and 101.9

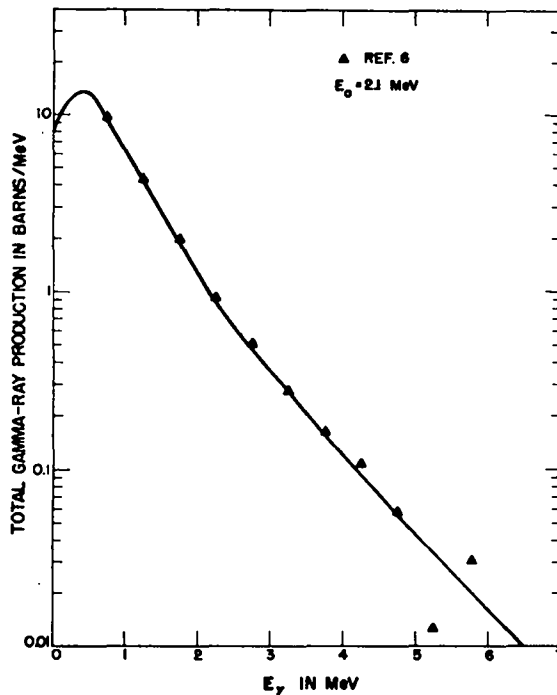
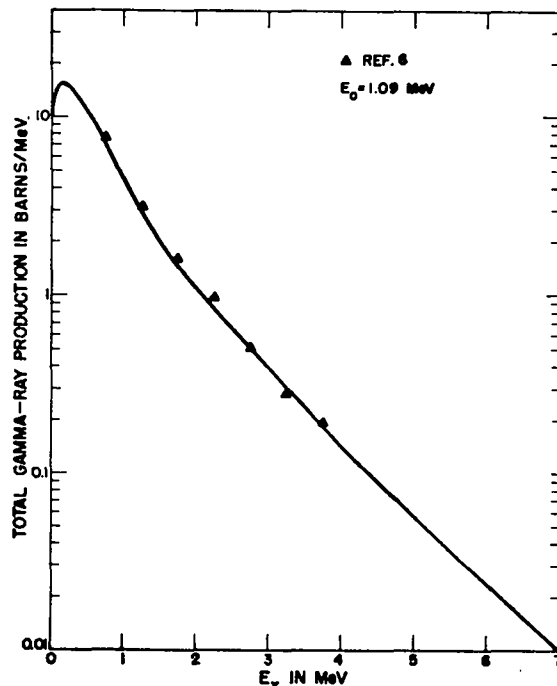


Fig. 4. Total gamma-ray production cross sections for  $^{238}\text{U}$  in barns per MeV as a function of  $E_{\gamma}$ , for incident neutrons of 1.09, 2.1,



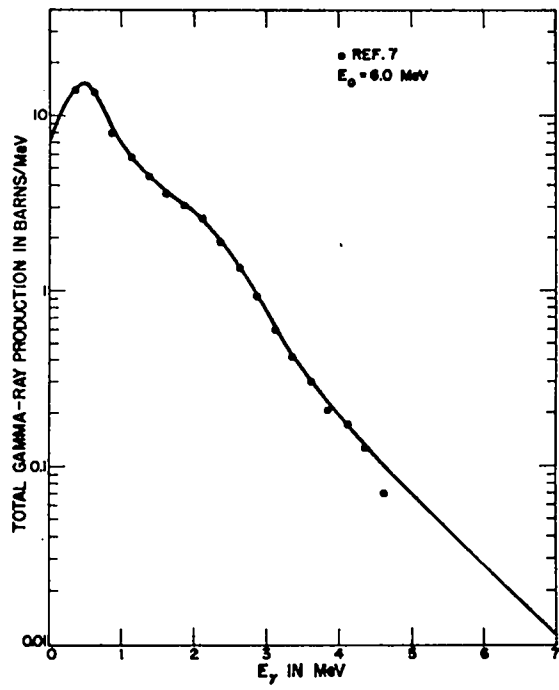
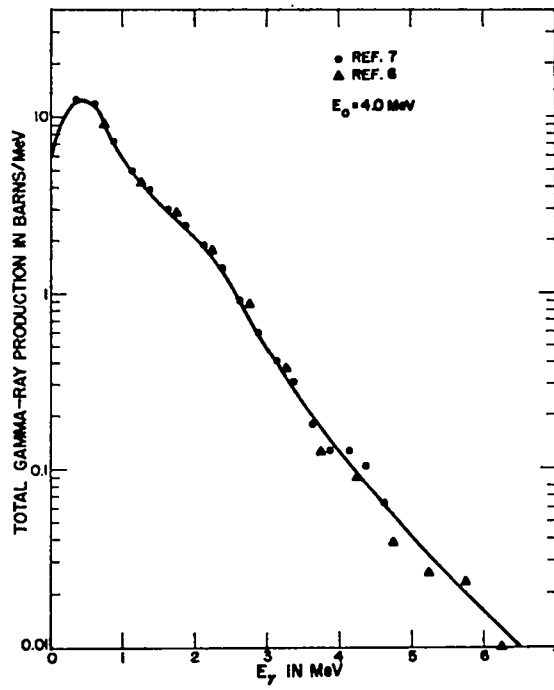
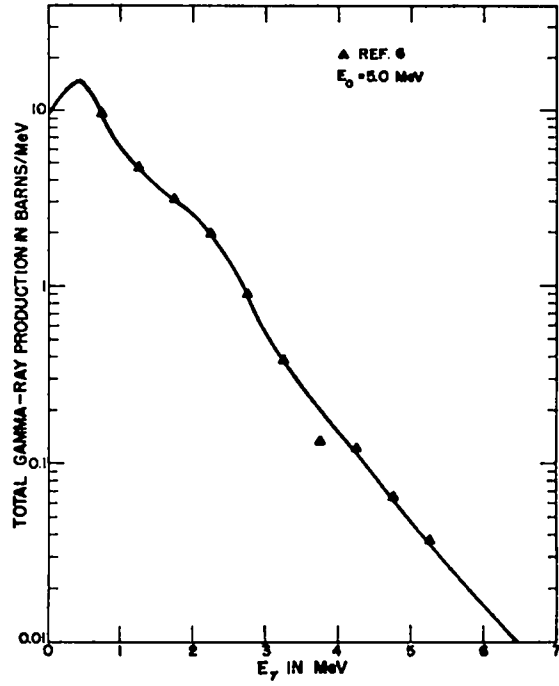
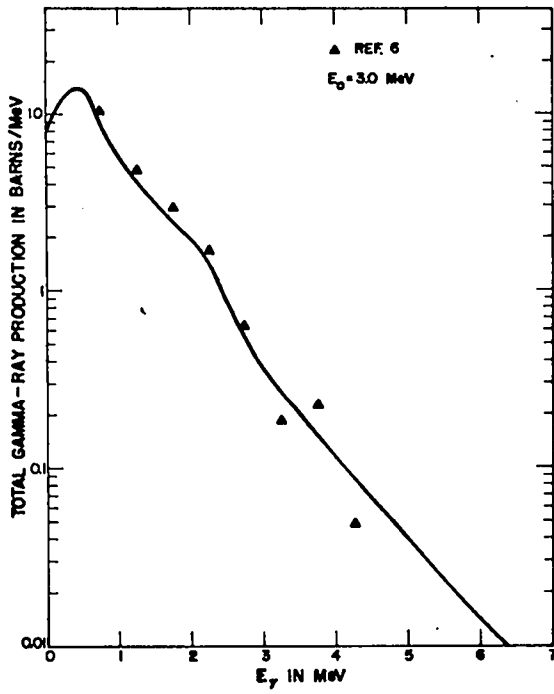
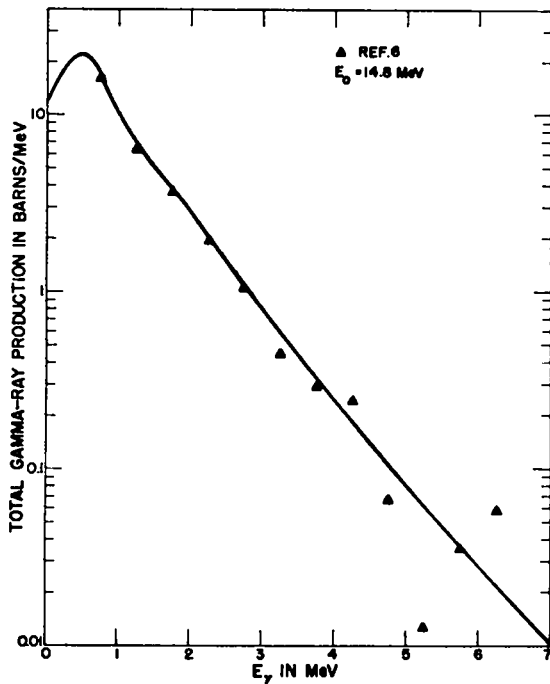
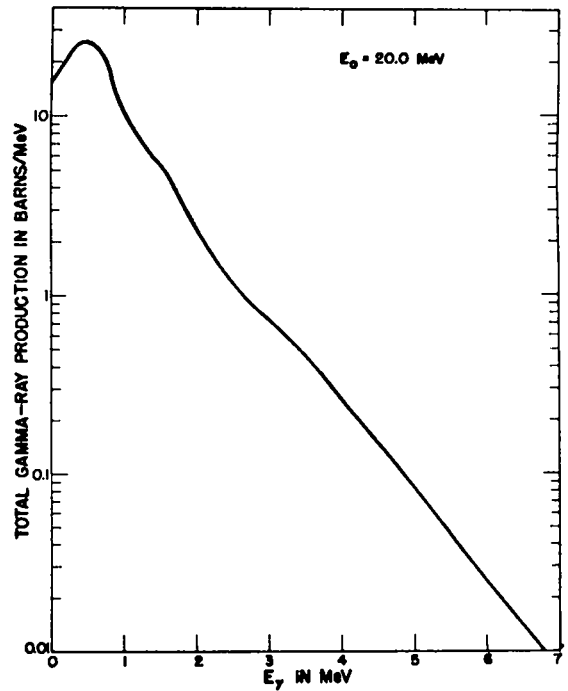
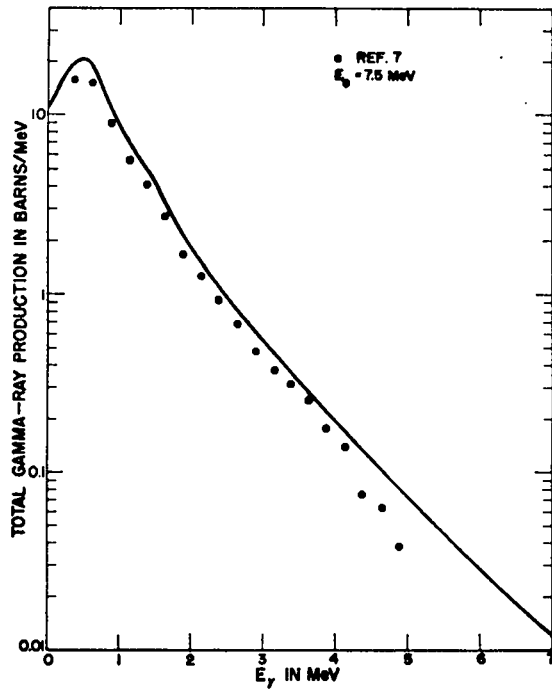


Fig. 4. (Cont) 3.0, 4.0, 5.0, 6.0



keV. These data are presented in Fig. 5 along with the evaluated curves chosen here. Although a number of references give some information on the resolved lines from radiative capture on  $^{238}\text{U}$ , both the resolved and continuum spectra are needed for a complete evaluation. Further, the experimental measurements must be reduced to the absolute number of photons per capture, or they must be given in absolute units such as barns/MeV; therefore few of the extant data could be used easily in this analysis. Therefore, the data\* of John and Orphan were chosen and were treated as follows.

The given experimental points were plotted in units of photons per MeV per capture and "eye-ball" curves were drawn through the data after adjustments were made to obtain the total binding energy (4.80 MeV), upon integration. These measurements

\*The LASL data of Jurney and Sheline<sup>5</sup> were not complete when this report was written. As soon as they become available, the  $^{238}\text{U}$  thermal capture spectrum will be modified accordingly.

Fig. 4. (Cont) 7.5, 14.8, and 20 MeV.

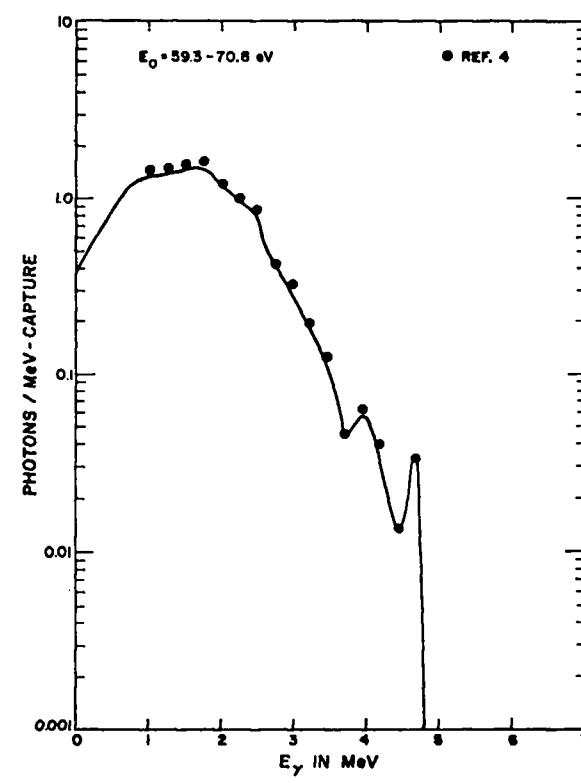
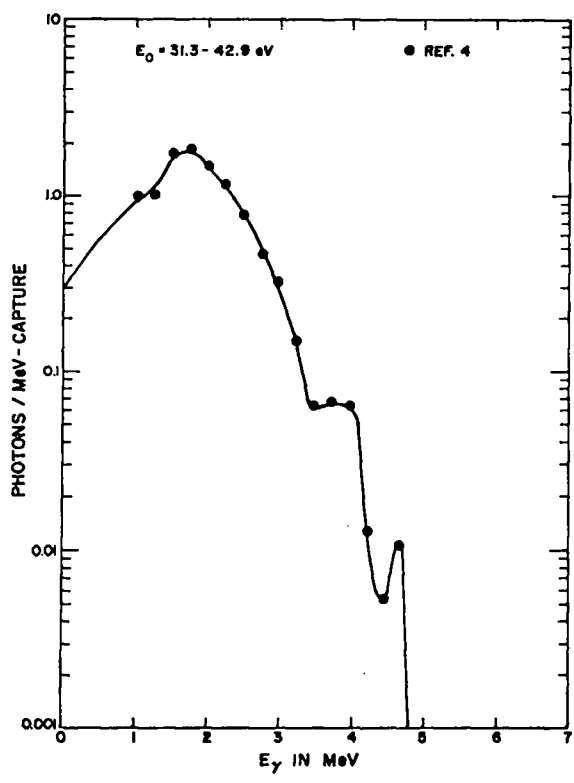
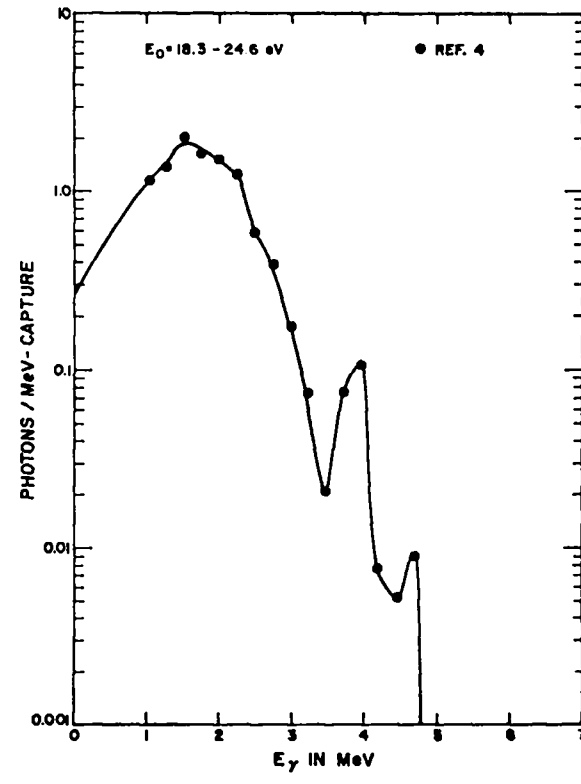
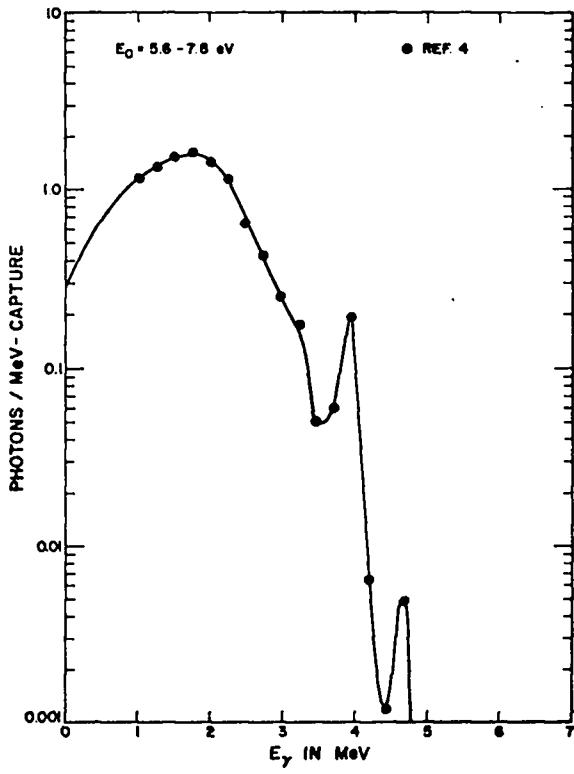


Fig. 5. Numbers of gamma-rays as a function of  $E_\gamma$  due to capture by  $^{238}\text{U}$  for incident neutrons with energies of 5.6 - 7.8 eV, 18.3 - 24.6 eV, 31.3 - 42.9 eV, 59.3 - 70.8 eV,

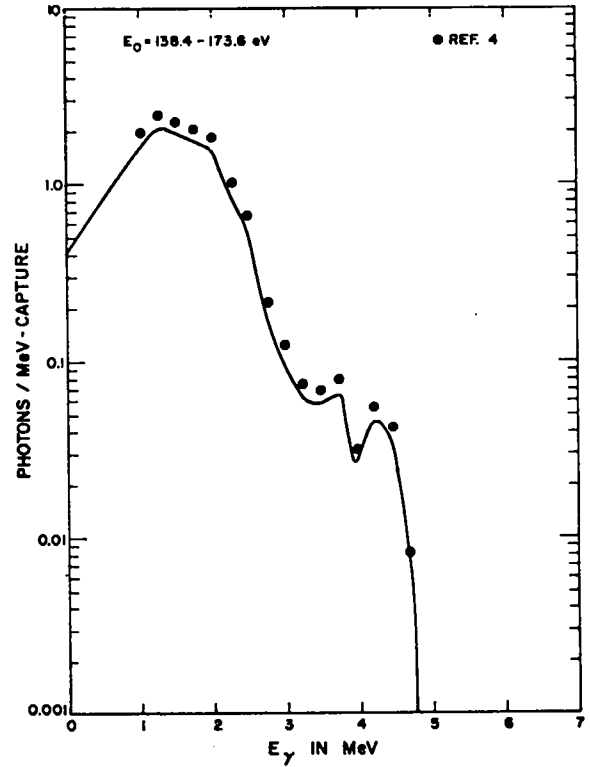
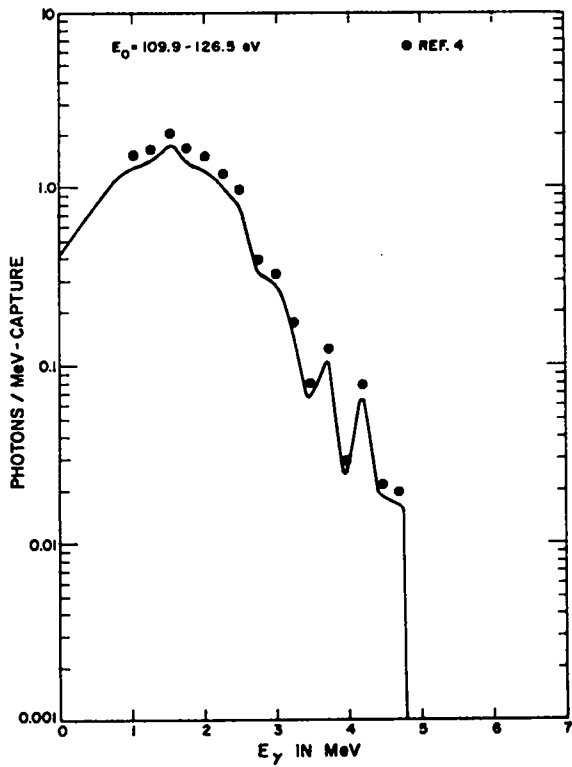
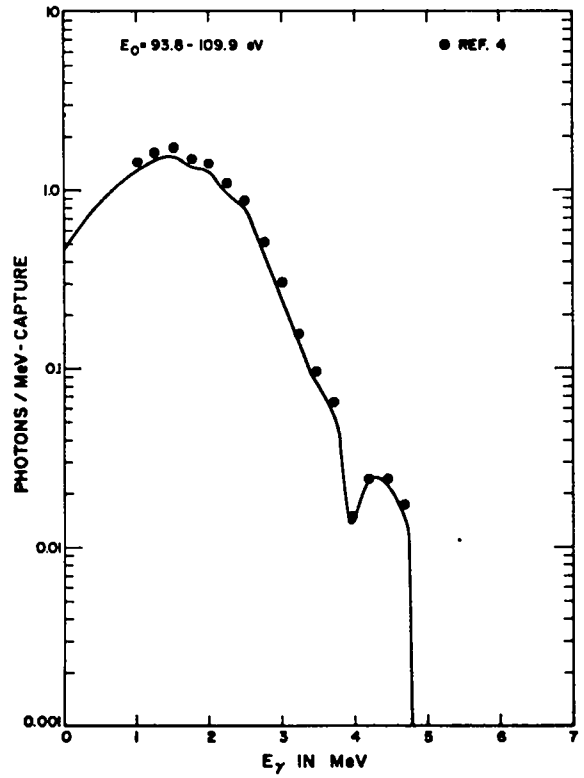
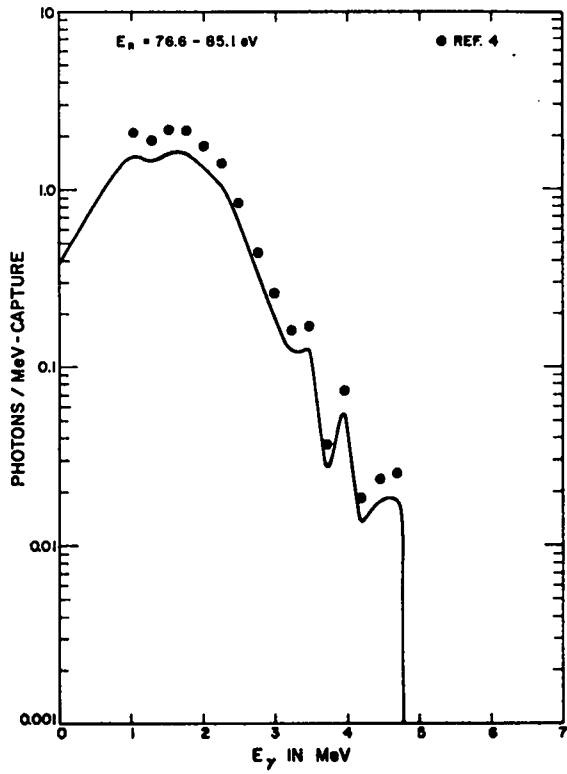


Fig. 5. (Cont) 76.6 - 85.1 eV, 93.8 - 109.9 eV, 109.9 - 126.5 eV, 138.4 - 173.6 eV,

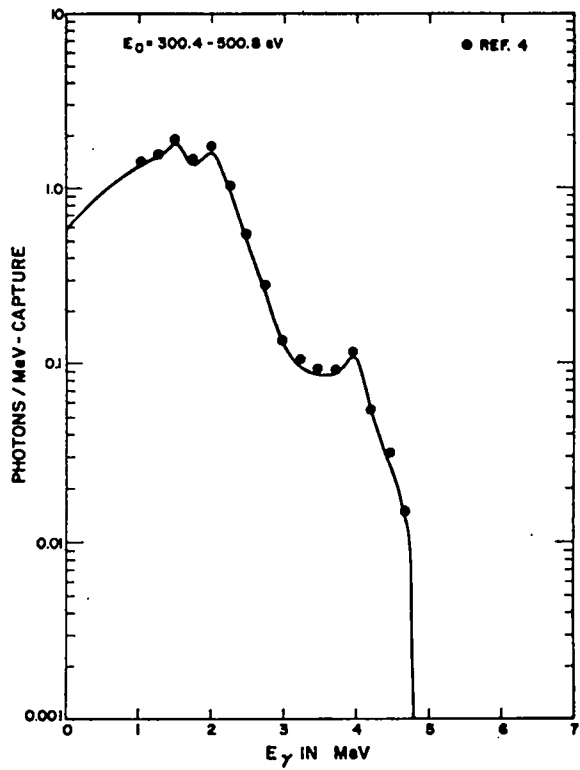
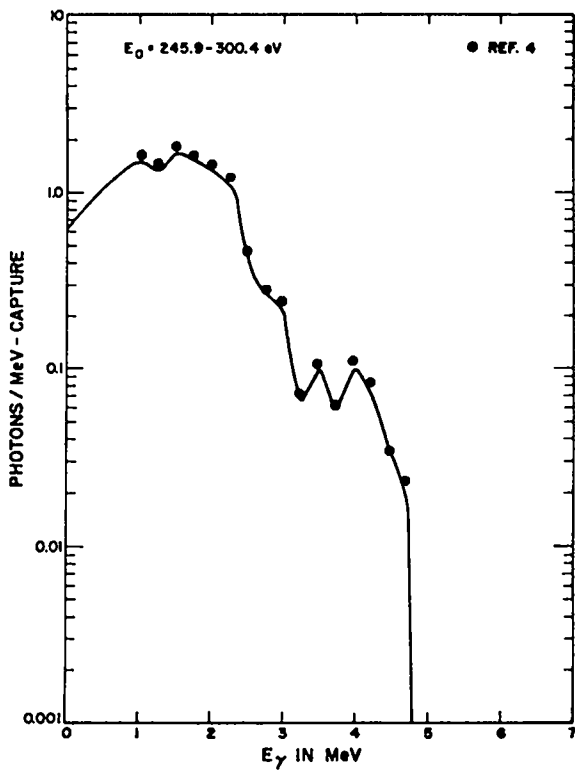
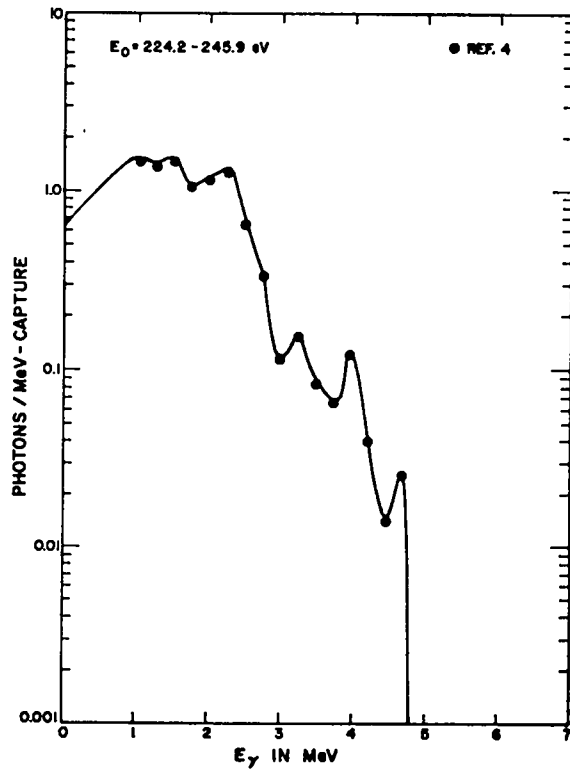
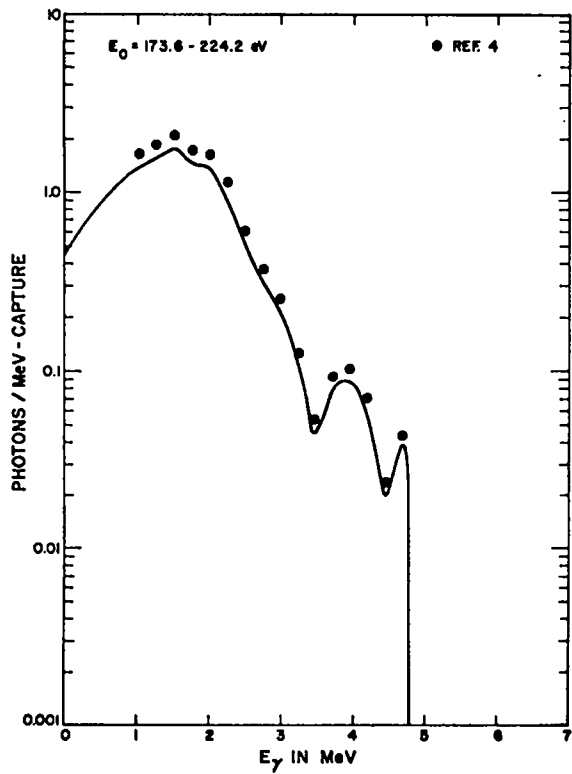


Fig. 5. (Cont) 173.6 - 224.2 eV, 224.2 - 245.9 eV, 245.9 - 300.4 eV, 300.4 - 500.8 eV,

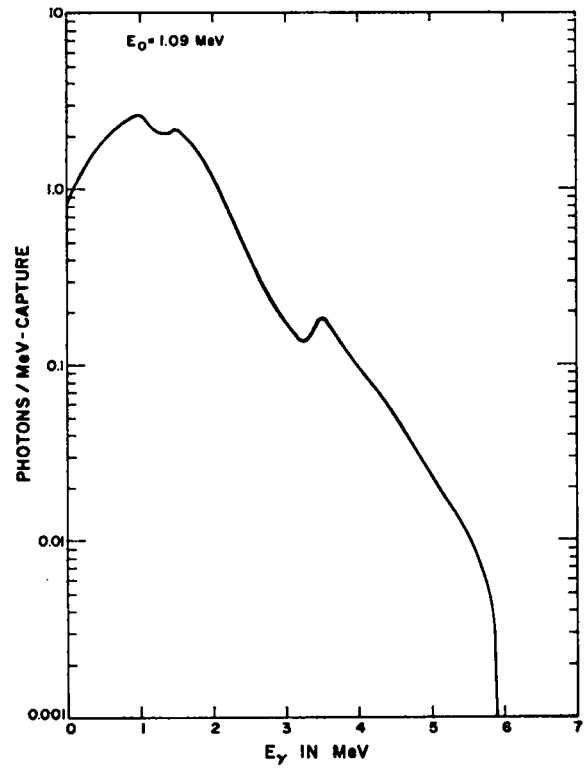
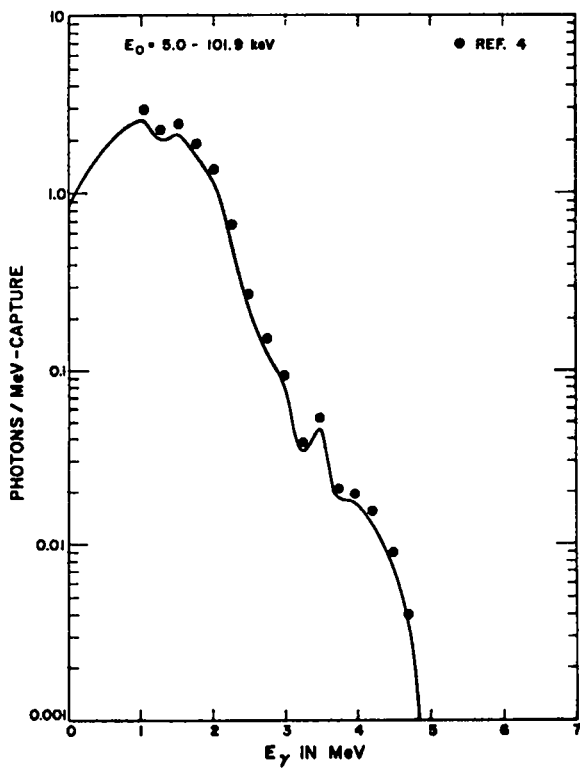
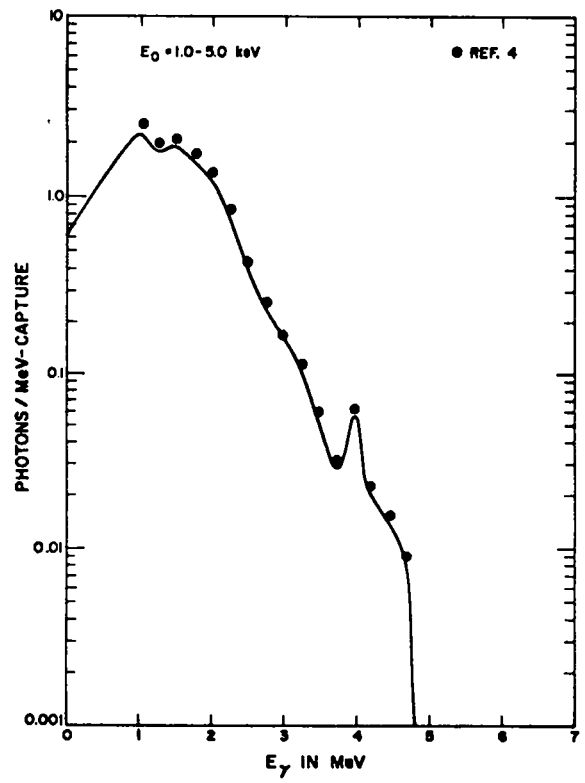
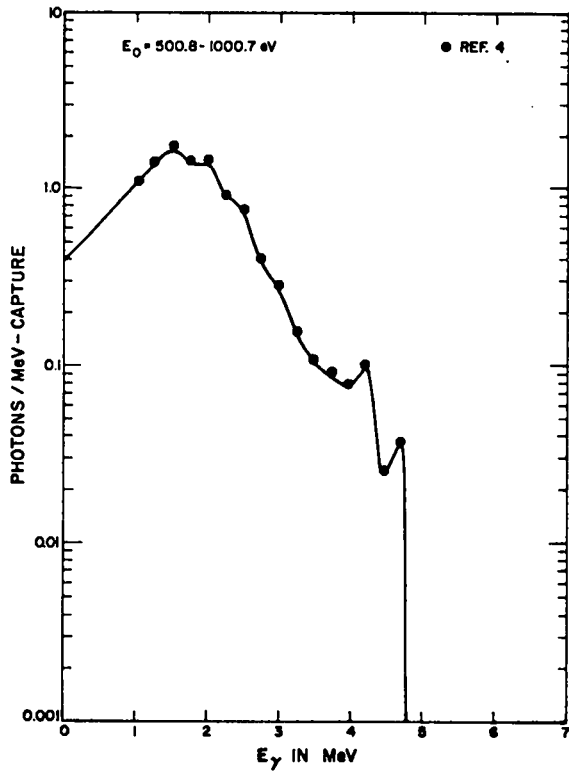


Fig. 5. (Cont) 500.8 - 1000.7 eV, 1.0 - 5.0 keV, 5.0 - 101.9 keV, and 1.09 MeV.

are presented for gamma rays above 900 keV in energy intervals of  $\sim 220$  keV. Perhaps two points should be made: First, John and Orphan report energy-balance errors that average about 6.5% and additional uncertainties of about 5.5%. Second, the extrapolation below  $E_\gamma = 900$  keV contributes significant uncertainties to the integral cross sections, spectra, and the evaluated multiplicities and energy balance obtained. Thus, these adjustments were typically about 7 - 10% but were well within the range of the experimental measurements and certainly within the calculational errors.

Multiplicities were obtained by integrating each curve over  $E_\gamma$  and then normalizing the curves to one photon per capture. The normalized curves should be used at the midpoint of each incident neutron energy interval with linear interpolation on the spectra and multiplicities between the energy ranges given. The lowest-energy distribution and multiplicity should be used for all incident neutron energies below that midpoint energy ( $E_0 = 6.7$  eV).

#### B. 45 keV to 1.09 MeV

##### 1. Radiative Capture

The midpoint energy for the highest-energy interval from the data of John and Orphan<sup>4</sup> is 53.5 keV; the curve and data for that energy are given in Fig. 5. This normalized spectrum was then hardened (somewhat arbitrarily) to balance the total energy available from capture ( $E_0 + E_b$ , or 5.89 MeV). This seemed a more reasonable step than simply raising the multiplicity. The calculated distribution is shown in the last part of Fig. 5 as photons/MeV per capture from which the multiplicity was obtained by integration.

## 2. Fission

It was assumed that the fission gamma-ray distribution for  $^{238}\text{U}$  is essentially the same as that for  $^{235}\text{U}$ . The curve for  $^{235}\text{U}$  is shown in Fig. 1. The normalized distribution, multiplicity, and total gamma-ray energy are thus assumed to be independent of incident neutron energy.

## 3. Inelastic Scattering

Gamma rays emitted from inelastic scattering were calculated in the same manner as those for  $^{235}\text{U}$ , taking inelastic neutron cross sections from the evaluation of Berlijn et al.<sup>13</sup> Gamma-ray decay schemes were obtained from the compilation given by Ellis.<sup>15</sup>

#### C. 1.09 to 20 MeV

Nellis and Morgan<sup>6</sup> have reported measurements of the total gamma-ray spectra at  $E_0 = 1.09, 2.1, 3.0, 4.0, 5.0,$  and  $14.8$  MeV. The smooth curves drawn through these data were checked against Eq. (1) and found to agree within the experimental errors involved. The shape of the curve for  $E_0 = 1.09$  MeV was adjusted at low gamma-ray energies to agree roughly with the total cross-section distributions calculated on the basis of the fission, capture, and inelastic scattering spectra discussed above.

The gamma-ray cross sections and spectra for  $^{238}\text{U}$  were extended to  $E_0 = 20$  MeV by extrapolating the data from lower energies. The experimental data and evaluated curves in barns/MeV are shown in Fig. 6.

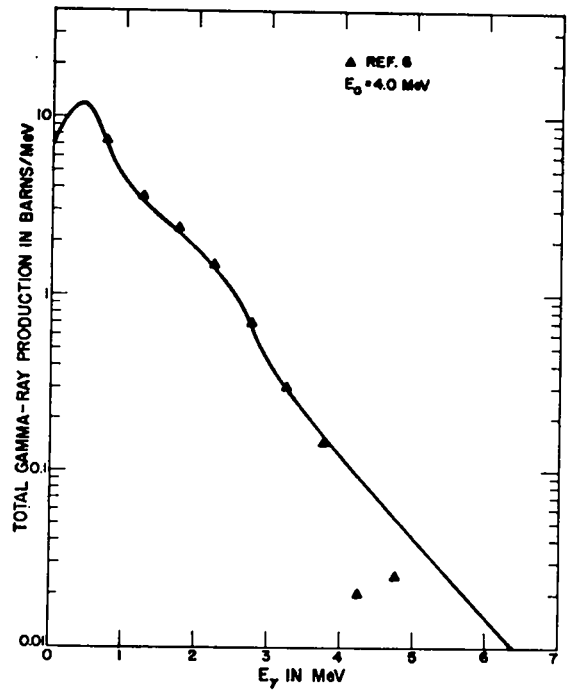
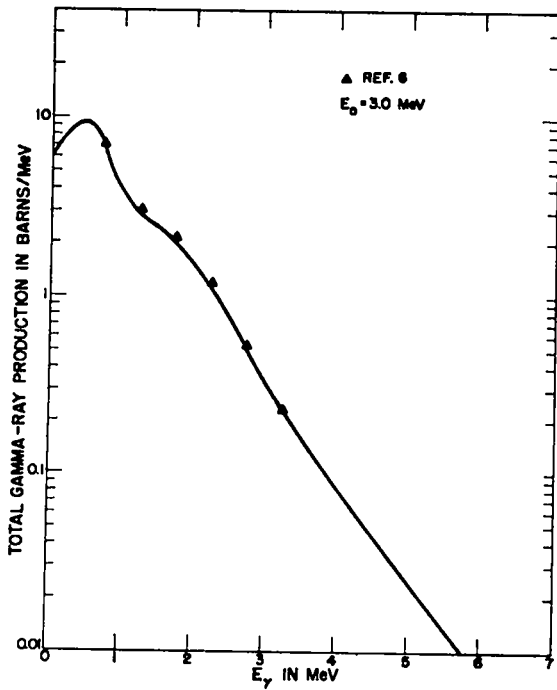
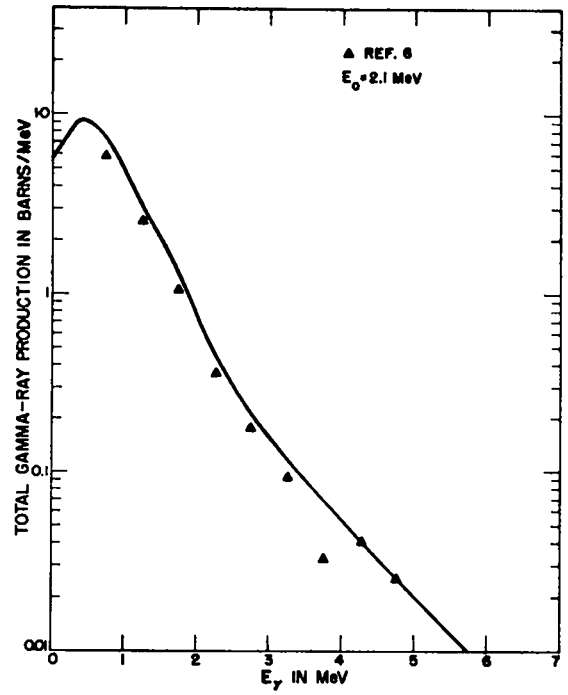
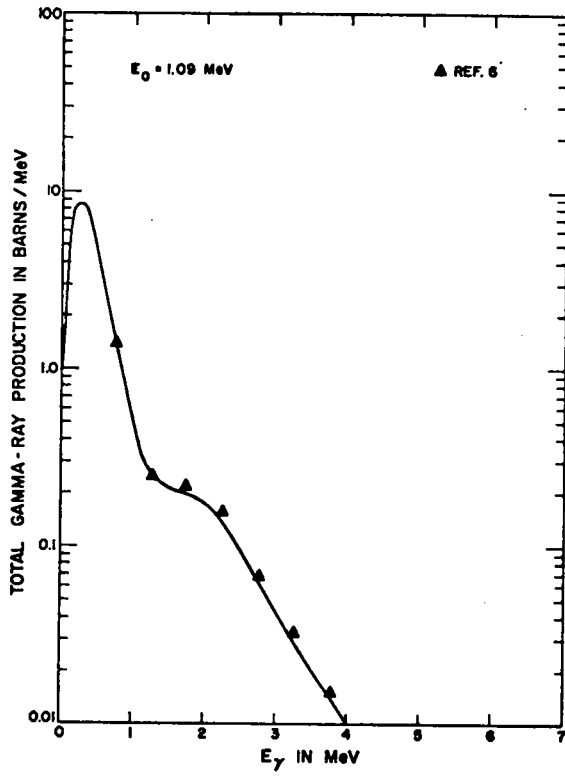


Fig. 6. Total gamma-ray production cross sections for  $^{238}\text{U}$  in barns per MeV as function of  $E_\gamma$ , for incident neutrons of 1.09, 2.1, 3.0, 4.0,



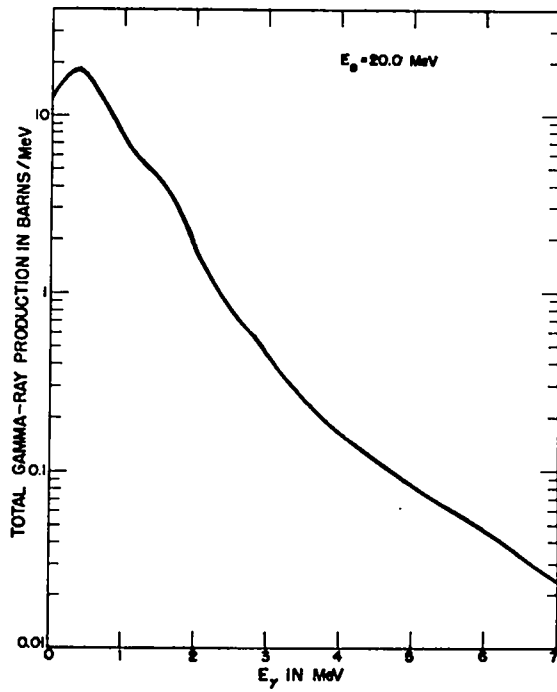
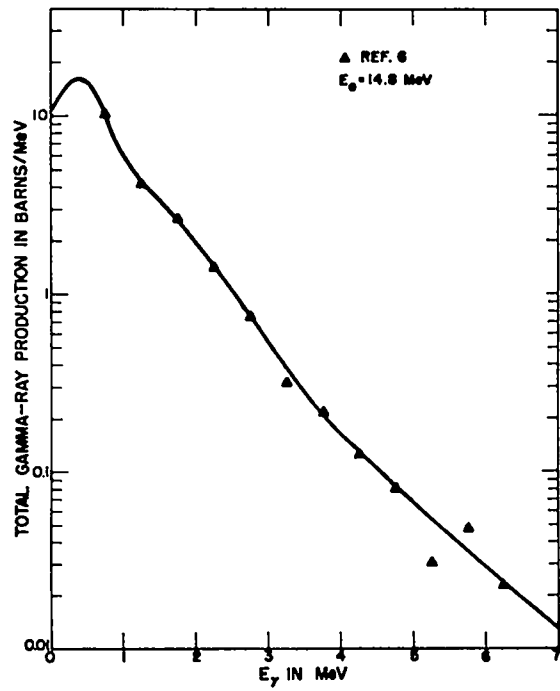
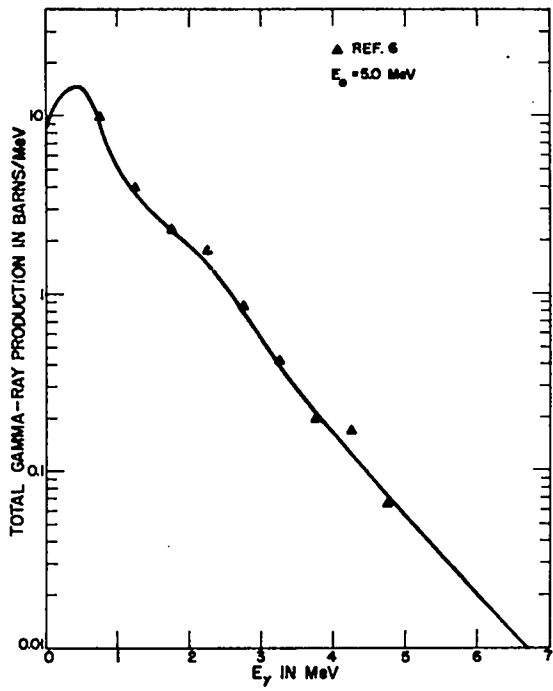


Fig. 6. (Cont) 5.0, 14.8, and 20.0.

#### IV. RESULTS

The final results are given in tabular form to facilitate input into a library file and to allow changes to be incorporated readily at a later date. The total gamma-ray production cross sections in barns, integrated over  $E_\gamma$ , are plotted as a function of incident neutron energy above 1 MeV for  $^{235}\text{U}$  and  $^{238}\text{U}$  in Fig. 7, the tabular results are listed separately.

Linear interpolation is recommended for the tabular data which follow, but it is recognized that some users may find it necessary to employ other interpolation schemes if required by their particular processing codes. In such cases, additional datum points (from the microscopic curves) and/or renormalization of probabilities may be necessary to ensure proper representation of the data. Note also that the energy mesh used for  $\sigma_{\text{Yprod}}(E_\gamma)$  and  $P(E_\gamma)$  does not necessarily coincide with the fine structure for the gamma-ray probability distribution for radiative capture for either  $^{235}\text{U}$  or  $^{238}\text{U}$  at thermal. The errors involved in failing to represent those peaks precisely are considerably less than the uncertainty in the gross distribution, because that curve was based on the radiative-capture process for hafnium and therefore may be systematically different from measurements on  $^{235}\text{U}$ . Further, preliminary thermal-capture data on  $^{238}\text{U}$  indicate that the major contributions come from line spectra.

Again the reader should note that all distributions except those on inelastic scattering (Tables IV and X) are given in units of probability per MeV or barns/MeV. The latter are presented as probabilities for the production of gamma rays of discrete energies,  $E_{\gamma i}$ , and/or total number of gamma

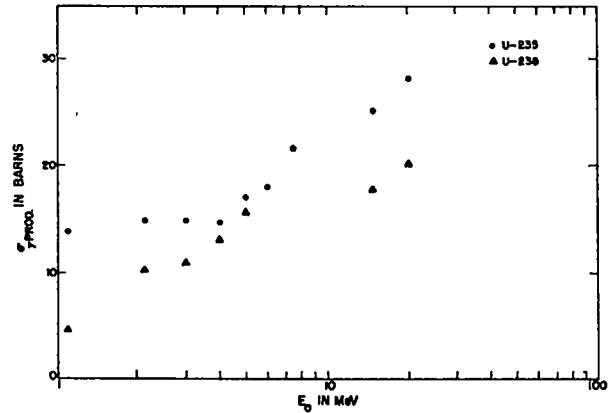


Fig. 7. Total gamma-ray production cross sections in barns for  $^{235}\text{U}$  and  $^{238}\text{U}$  as a function of incident neutron energy from 1 to 20 MeV.

rays in energy intervals,  $\Delta E_\gamma$ . Quoting probability per MeV for a discrete level is physically meaningless unless some specification of line width and shape is given. The tabular results for both  $^{235}\text{U}$  and  $^{238}\text{U}$  are presented in Tables I through XIII at the end of this report.

#### V. DISCUSSION

The question of time dependence of gamma-ray spectra and total energy was discussed in some detail in Ref. 1. It should be repeated here that the gamma rays treated in this report are assumed to be emitted within 100 nsec after scission; that is, all capture, prompt fission, and inelastic processes are short-lived. This choice of time interval separates (approximately) direct and cascade gamma decays from those which follow beta decays from fission and whose decay times, on the average, are much longer. No account has been taken of the isomeric gammas.

Note that the total gamma-ray energies for the two time intervals ( $< 100$  nsec and  $> 100$  nsec) are approximately equal. For some reactor problems,

these processes could be of equal importance. At some later date, the time dependence of the fission gamma-ray spectra may be considered for input calculations.

The time dependence of the fission gamma-ray spectrum on incident neutron energy over all times has not been established, although Sund and Verbinski<sup>16</sup> have recently reported isomeric data covering times up to 1  $\mu$ sec following thermal fission of  $^{235}\text{U}$ . As the incident neutron energy changes, the spectrum may change considerably owing to variation of the fission products. Their data,<sup>16</sup> for example, indicate much softer spectra than assumed here for the prompt gammas.

#### ACKNOWLEDGMENTS

We gratefully acknowledge the contributions of E. T. Journey, R. K. Sheline, P. P. Whalen, and H. T. Motz to the various aspects of this effort. We also thank T. J. Hirons, D. W. Watkins, and T. L. Talley for their many helpful comments on the presentation of the results. Finally, without the support and encouragement of C. C. Cremer, we would not have embarked on this program.

#### REFERENCES

1. R. E. Hunter and L. Stewart, "An Evaluation of the Neutron-Induced Gamma-Ray Production Cross Sections for Pu-239 and Pu-249." Los Alamos Scientific Laboratory report LA-4901.
2. V. V. Verbinski and R. E. Sund, "Measurement of Prompt Gamma-Rays from Thermal-Neutron Fission of  $^{235}\text{U}$  and  $^{239}\text{Pu}$ , and from Spontaneous Fission of  $^{252}\text{Cf}$ ," Gulf Radiation Technology report GA-9148 (1969).
3. R. W. Peelle and F. C. Maienschein, "The Absolute Spectrum of Photons Emitted in Coincidence with Thermal-Neutron Fission of Uranium-235," Oak Ridge National Laboratory report ORNL-4457 (1970).
4. J. John and V. J. Orphan, "Gamma Rays from Resonant Capture of Neutrons in  $^{238}\text{U}$ ," Gulf Radiation Technology report GA-10196 (1970).

5. E. T. Journey, private communication (1971).
6. D. O. Nellis and I. L. Morgan, "Gamma-Ray Production Cross Sections for  $\text{U}^{235}$ ,  $\text{U}^{238}$ , and  $\text{Pu}^{239}$ ," Texas Nuclear Corporation report ORO-2791-17 (1966); also reported in P. S. Buchanan, "A Compilation of Cross Sections and Angular Distributions of Gamma Rays Produced by Neutron Bombardment of Various Nuclei," Texas Nuclear Corporation report ORO-2791-28 (1969).
7. D. M. Drake, "Inelastic Neutron Scattering and Gamma Production from Fast-Neutron Bombardment of  $^{235}\text{U}$ ," Nucl. Phys. A133, 108 (1969).
8. E. T. Journey and R. K. Sheline, private communication, (1971).
9. V. J. Orphan, N. C. Rasmussen, and T. L. Harper, "Line and Continuum Gamma-Ray Yields from Thermal-Neutron Capture in 75 Elements," Gulf Radiation Technology report GA-10248 (1970).
10. F. C. Maienschein, R. W. Peelle, W. Zobel, and T. A. Love, "Gamma Rays Associated with Fission," Proc. U. N. Inter. Conf. Peaceful Uses of Atomic Energy, 2nd, Geneva, 1958, 15, 366 (1958).
11. F. E. W. Rau, "Ausbeute an Prompter Gammastrahlung bei Spaltung von Uran 235 durch Thermische Neutronen," Ann. Physik (7) 10, 252 (1963).
12. M. F. James, "Energy Released in Fission," J. Nucl. Energy 23, 517 (1969).
13. J.-J. H. Berlijn, R. E. Hunter, and C. C. Cremer, "Neutron Cross Sections for  $^{235}\text{U}$  and  $^{238}\text{U}$  in the Energy Range 1 keV to 14 MeV," Los Alamos Scientific Laboratory report LA-3527 (1968).
14. C. M. Lederer, J. M. Hollander, and J. Perlman, Table of Isotopes, 6th Ed., John Wiley & Sons, New York (1967).
15. Y. A. Ellis, "Nuclear Data Sheets for A = 238," Nuclear Data, Sect. B 4, 635 (1970).
16. R. E. Sund and V. V. Verbinski, "Measurement of Isomeric Gamma Rays from Fission for Times Less Than One Microsecond after Fission," Gulf Radiation Technology report RT-C9366 (1971).

TABLE I

PROBABILITY FOR FISSION GAMMA RAYS  
FOR  $^{235}\text{U}$  AND  $^{238}\text{U}$   
(Normalized to One Photon per Fission)  
 $E_0 = 10^{-5}$  eV to 1.09 MeV

$E_\gamma$ (MeV)	$P(E_\gamma)$ Prob/MeV	$E_\gamma$ (MeV)	$P(E_\gamma)$ Prob/MeV	$E_\gamma$ (MeV)	$P(E_\gamma)$ Prob/MeV
0.0	0.1416	0.575	0.8750	3.25	0.0248
0.05	0.2365	0.605	0.9529	3.5	0.0197
0.10	0.3950	0.625	0.8623	3.75	0.0156
0.15	0.6669	0.65	0.7278	4.0	0.0127
0.163	0.7094	0.67	0.7745	4.25	0.00934
0.178	0.6117	0.683	0.7986	4.5	0.00657
0.20	0.8623	0.70	0.7179	4.75	0.00507
0.212	1.1044	0.75	0.6966	5.0	0.00421
0.225	0.8425	0.80	0.6626	5.25	0.00355
0.245	0.6088	0.90	0.5097	5.5	0.00302
0.265	0.4106	1.00	0.4205	5.75	0.00258
0.30	0.6839	1.10	0.3582	6.0	0.00217
0.325	0.8170	1.20	0.3412	6.25	0.00176
0.35	1.0294	1.25	0.3271	6.5	0.00142
0.365	1.0648	1.35	0.2818	6.75	0.00110
0.40	0.9387	1.50	0.2011	7.0	0.00086
0.43	0.8410	1.75	0.1288	7.25	0.00064
0.45	0.8835	2.0	0.0934	7.5	0.00042
0.485	0.9954	2.25	0.0736	7.75	0.00012
0.50	0.9586	2.5	0.0586	8.0	0.00001
0.525	0.8241	2.75	0.0450	8.1	0.0
0.545	0.7320	3.0	0.0343		

TABLE II

PROBABILITY FOR RADIATIVE-CAPTURE GAMMA RAYS  
FOR  $^{235}\text{U}$   
(Normalized to One Photon per Capture)  
 $E_0 = 10^{-5}$  eV to 13 keV

$E_\gamma$ (MeV)	$P(E_\gamma)$ Prob/MeV	$E_\gamma$ (MeV)	$P(E_\gamma)$ Prob/MeV	$E_\gamma$ (MeV)	$P(E_\gamma)$ Prob/MeV
0.0	0.106	1.0	0.345	3.5	0.0796
0.1	0.549	1.25	0.425	3.75	0.0669
0.2	0.510	1.5	0.374	4.0	0.0488
0.3	0.343	1.75	0.310	4.25	0.0446
0.4	0.271	2.0	0.254	4.5	0.0308
0.5	0.229	2.25	0.234	4.75	0.0244
0.6	0.209	2.5	0.195	5.0	0.0212
0.7	0.213	2.75	0.154	5.5	0.0393
0.8	0.231	3.0	0.125	6.0	0.0117
0.9	0.270	3.25	0.0945	6.5	0.0011

TABLE III

PROBABILITY FOR RADIATIVE-CAPTURE GAMMA RAYS  
FOR  $^{235}\text{U}$   
(Normalized to One Photon per Capture)  
 $E_0 = 1.09$  MeV

$E_\gamma$ (MeV)	$P(E_\gamma)$ Prob/MeV	$E_\gamma$ (MeV)	$P(E_\gamma)$ Prob/MeV	$E_\gamma$ (MeV)	$P(E_\gamma)$ Prob/MeV
0.0	0.0944	1.0	0.307	3.5	0.102
0.1	0.488	1.25	0.376	3.75	0.0892
0.2	0.453	1.5	0.331	4.0	0.0737
0.3	0.305	1.75	0.262	4.25	0.0662
0.4	0.241	2.0	0.223	4.5	0.0540
0.5	0.204	2.25	0.208	4.75	0.0471
0.6	0.186	2.5	0.190	5.0	0.0420
0.7	0.190	2.75	0.166	5.5	0.0727
0.8	0.206	3.0	0.144	6.0	0.0223
0.9	0.240	3.25	0.122	6.5	0.0135
				7.0	0.0045

TABLE IV

MULTIPLICITIES FOR GAMMA-RAY PRODUCTION FROM INELASTIC SCATTERING ON  $^{235}\text{U}$  $E_0 = 13 \text{ keV to } 1.09 \text{ MeV.}$ 

$E_0$ (keV) \ $E_\gamma$ (keV)	Total Multi- plicities	13	39	52	69	98	103	115	119
13.055	1.000	1.000							
52.218	1.000	1.000	0.0	0.0					
82.344	1.1921	0.4778	0.1917	0.5226	0.0				
103.433	1.2819	0.4446	0.2039	0.5553	0.0781		0.0		
150.630	1.4247	0.4670	0.2132	0.5668	0.1709	0.0	0.0068		
171.718	1.4378	0.4579	0.1976	0.5649	0.1927	0.0181	0.0066		0.0
197.827	1.4635	0.4633	0.1940	0.5578	0.2132	0.0240	0.0080	0.0	0.0016
225.945	1.4912	0.4666	0.1860	0.5394	0.2325	0.0279	0.0078	0.0170	0.0078
296.239	1.5701	0.4167	0.1944	0.5599	0.2193	0.0322	0.0073	0.0307	0.0497
334.400	1.5773	0.4349	0.1836	0.5351	0.2160	0.0565	0.0085	0.0424	0.0607
368.541	1.7381	0.4373	0.1984	0.5309	0.2082	0.0852	0.0070	0.0433	0.0685
395.655	1.7979	0.4080	0.1756	0.5269	0.2047	0.1065	0.0111	0.0581	0.0802
415.739	1.7914	0.3999	0.1751	0.5144	0.1944	0.1214	0.0083	0.0593	0.0731
428.793	1.8768	0.4090	0.1778	0.5185	0.1874	0.1094	0.0082	0.0616	0.0848
475.991	1.8753	0.3991	0.1691	0.4938	0.1732	0.1137	0.0081	0.0636	0.0771
500.0	1.9549	0.3896	0.1848	0.5061	0.1687	0.1285	0.0094	0.0603	0.0763
535.239	1.9348	0.3937	0.1696	0.4986	0.1606	0.1217	0.0091	0.0596	0.0699
600.0	2.1312	0.4044	0.1812	0.4992	0.1704	0.1824	0.0072	0.0636	0.0660
654.738	2.2333	0.3980	0.1698	0.4921	0.1801	0.2042	0.0057	0.0688	0.0631
700.0	2.2346	0.4136	0.1555	0.4478	0.1721	0.2052	0.0055	0.0596	0.0563
774.238	2.2456	0.4306	0.1435	0.4092	0.1741	0.1965	0.0061	0.0641	0.0489
800.0	2.2510	0.4367	0.1365	0.3986	0.1667	0.1998	0.0050	0.0602	0.0482
900.0	2.1684	0.4200	0.1237	0.3535	0.1412	0.1791	0.0055	0.0545	0.0378
1000.0	2.0411	0.3834	0.1080	0.3128	0.1198	0.1572	0.0051	0.0484	0.0323
1090.0	2.1285	0.4106	0.1134	0.3295	0.1349	0.1656	0.0058	0.0563	0.0339
Excitation Energy (keV)	<u>All</u>	<u>13</u>	<u>52</u>	<u>52</u>	<u>82</u>	<u>150</u>	<u>103</u>	<u>197</u>	<u>171</u>
$E_0$ (keV) \ $E_\gamma$ (keV)	144	162	171	189	196	311	315	324	333
171.718			0.0						
197.827			0.0016						
225.945			0.0062						
296.239	0.0		0.0599						
334.400	0.0198	0.0	0.0918						0.0
368.541	0.0224	0.0056	0.1271		0.0		0.0		0.0042
395.655	0.0443	0.0194	0.1355		0.0055		0.0028		0.0138
415.739	0.0469	0.0193	0.1296	0.0	0.0083	0.0	0.0041		0.0152
428.793	0.0506	0.0192	0.1436	0.0055	0.0287	0.0014	0.0123		0.0150
475.991	0.0636	0.0311	0.1394	0.0122	0.0176	0.0041	0.0081	0.0	0.0230
500.0	0.0683	0.0375	0.1754	0.0134	0.0134	0.0040	0.0054	0.0054	0.0281
535.239	0.0544	0.0298	0.1709	0.0181	0.0194	0.0065	0.0091	0.0155	0.0220
600.0	0.0732	0.0444	0.1524	0.0180	0.0144	0.0060	0.0096	0.0300	0.0432
654.738	0.0734	0.0447	0.1548	0.0184	0.0172	0.0057	0.0069	0.0436	0.0516
700.0	0.0717	0.0441	0.1434	0.0176	0.0165	0.0055	0.0077	0.0386	0.0574
774.238	0.0662	0.0387	0.1272	0.0163	0.0153	0.0061	0.0071	0.0387	0.0540
800.0	0.0643	0.0392	0.1205	0.0151	0.0151	0.0050	0.0070	0.0382	0.0572
900.0	0.0554	0.0342	0.1043	0.0166	0.0157	0.0055	0.0065	0.0351	0.0517
1000.0	0.0476	0.0298	0.0926	0.0178	0.0162	0.0060	0.0068	0.0306	0.0468
1090.0	0.0464	0.0290	0.0960	0.0174	0.0166	0.0058	0.0075	0.0298	0.0488
Excitation Energy (keV)	<u>295</u>	<u>333</u>	<u>171</u>	<u>414</u>	<u>367</u>	<u>414</u>	<u>367</u>	<u>474</u>	<u>333</u>

TABLE IV (cont)

$E_Y$ (keV) $E_0$ (keV)	342	367	375	381	394	414	422	451	639
368.541		0.0							
395.655	0.0	0.0055		0.0	0.0				
415.739	0.0014	0.0083		0.0041	0.0083				
428.793	0.0027	0.0274	0.0	0.0041	0.0096	0.0			
475.991	0.0081	0.0257	0.0068	0.0108	0.0203	0.0068	0.0		
500.0	0.0107	0.0241	0.0080	0.0080	0.0161	0.0080	0.0054		
535.239	0.0104	0.0220	0.0117	0.0117	0.0233	0.0117	0.0155	0.0	
600.0	0.0096	0.0168	0.0132	0.0384	0.0216	0.0120	0.0312	0.0228	
654.738	0.0115	0.0321	0.0138	0.0585	0.0229	0.0138	0.0447	0.0379	0.0
700.0	0.0132	0.0309	0.0154	0.0717	0.0232	0.0154	0.0386	0.0474	0.0331
774.238	0.0193	0.0285	0.0316	0.0702	0.0224	0.0305	0.0387	0.0478	0.0631
800.0	0.0171	0.0271	0.0321	0.0783	0.0221	0.0321	0.0382	0.0532	0.0673
900.0	0.0166	0.0286	0.0277	0.0748	0.0212	0.0277	0.0342	0.0508	0.0748
1000.0	0.0110	0.0298	0.0255	0.0706	0.0230	0.0255	0.0306	0.0468	0.0740
1090.0	0.0116	0.0298	0.0166	0.0762	0.0232	0.0166	0.0306	0.0513	0.0745
Excitation Energy (keV)	<u>394</u>	<u>367</u>	<u>427</u>	<u>394</u>	<u>394</u>	<u>427</u>	<u>474</u>	<u>533</u>	<u>652</u>

$E_Y$ (keV) $E_0$ (keV)	652	719	758	771
654.738	0.0			
700.0	0.0276			
774.238	0.0509	0.0	0.0	0.0
800.0	0.0552	0.0020	0.0030	0.0100
900.0	0.0618	0.0157	0.0231	0.0711
1000.0	0.0604	0.0255	0.0382	0.1190
1090.0	0.0613	0.0265	0.0397	0.1233
Excitation Energy (keV)	<u>652</u>	<u>771</u>	<u>771</u>	<u>771</u>

TABLE V

GAMMA-RAY MULTIPLICITIES FOR  $^{235}\text{U}$ ,  $10^{-5}$  eV to 1.09 MeV

$E_0$ (keV)	Fission	Radiative Capture	Inelastic
Thermal	7.17	3.73	0.0
13.055	7.17	3.73	1.0
52.2	7.17	3.73	1.0
82.3	7.17	3.73	1.192
103.4	7.17	3.73	1.282
150.6	7.17	3.73	1.425
197.8	7.17	3.73	1.464
225.9	7.17	3.73	1.491
296.2	7.17	3.73	1.570
334.4	7.17	3.73	1.649
368.5	7.17	3.73	1.738
395.7	7.17	3.73	1.798
428.8	7.17	3.73	1.877
500.0	7.17	3.73	1.955
600.0	7.17	3.73	2.131
700.0	7.17	3.73	2.235
800.0	7.17	3.73	2.251
1090.0 <sup>a</sup>	7.17	3.73	

<sup>a</sup> For  $E_0 > 1.09$  MeV, use the gamma-ray production cross sections in barns/MeV provided in Table VI.

TABLE VI

GAMMA-RAY PRODUCTION CROSS SECTIONS FOR  $^{235}\text{U}$  in Barns/MeV

$E_0$ (MeV) $E_\gamma$ (MeV)	1.09	2.1	3.0	4.0	5.0	6.0	7.5	14.8	20.0
0.0	9.77	8.14	8.02	5.89	9.36	7.04	10.09	11.86	14.75
0.1	15.26	10.13	9.73	8.18	11.02	8.92	12.68	14.38	17.50
0.2	15.56	11.57	11.09	10.28	12.39	10.80	15.39	16.90	20.28
0.3	14.26	13.06	12.20	11.62	13.85	12.98	18.09	19.84	23.57
0.4	12.66	13.82	12.88	12.27	14.73	14.57	19.94	21.73	25.61
0.5	11.07	13.44	12.80	12.07	14.24	15.16	20.80	21.94	25.55
0.6	9.37	12.21	11.60	11.67	12.78	14.27	19.57	21.10	24.79
0.7	7.78	10.32	9.64	9.98	10.44	11.89	16.12	19.00	22.91
0.8	6.46	8.46	8.11	8.18	8.53	9.91	13.05	15.33	18.35
0.9	5.33	7.19	6.67	6.93	7.12	8.23	10.71	11.86	13.61
1.0	4.39	6.22	5.78	5.94	6.14	7.07	8.90	9.80	11.00
1.25	2.87	4.07	4.04	4.24	4.60	5.13	5.88	6.72	7.32
1.50	1.97	2.73	3.15	3.23	3.68	4.03	4.25	5.13	5.50
1.75	1.42	1.85	2.48	2.57	3.01	3.35	2.68	3.78	3.69
2.00	1.09	1.26	1.92	2.06	2.48	2.82	1.83	2.82	2.43
2.25	0.828	0.866	1.42	1.58	1.94	2.18	1.32	2.04	1.63
2.50	0.658	0.641	0.853	1.15	1.38	1.63	0.981	1.50	1.18
2.75	0.509	0.479	0.538	0.724	0.878	1.12	0.729	1.09	0.916
3.00	0.395	0.366	0.360	0.486	0.556	0.751	0.551	0.800	0.743
3.25	0.307	0.274	0.266	0.334	0.371	0.504	0.416	0.586	0.587
3.50	0.238	0.209	0.204	0.238	0.276	0.347	0.321	0.436	0.459
3.75	0.184	0.158	0.152	0.196	0.204	0.252	0.246	0.324	0.343
4.00	0.144	0.122	0.115	0.123	0.154	0.196	0.190	0.245	0.258
4.25	0.114	0.093	0.088	0.094	0.113	0.146	0.149	0.185	0.196
4.50	0.091	0.072	0.067	0.071	0.086	0.115	0.116	0.140	0.147
4.75	0.072	0.055	0.051	0.054	0.064	0.088	0.090	0.106	0.111
5.00	0.058	0.043	0.040	0.042	0.048	0.069	0.071	0.082	0.083
5.50	0.037	0.026	0.023	0.025	0.027	0.043	0.044	0.048	0.045
6.00	0.029	0.016	0.014	0.016	0.016	0.028	0.029	0.028	0.025
6.50	0.015	0.009	0.008	0.010	0.009	0.018	0.018	0.017	0.014
7.0	0.010	0.007	0.006	0.0	0.005	0.011	0.012	0.010	0.007
8.0	0.0	0.0	0.0	0.0	0.0	0.0	0.0	0.0	0.0

TABLE VII

TOTAL GAMMA-RAY PRODUCTION CROSS SECTIONS FOR  $^{235}\text{U}$ 

$E_0$ (MeV)	$\int_0^{8.0 \text{ MeV}} \sigma_{\text{prod.}}(E_\gamma) dE_\gamma$	$\int_0^{0.5 \text{ MeV}} \sigma_{\text{prod.}}(E_\gamma) dE_\gamma$
	(barns)	(barns)
1.09	13.82	6.83
2.1	14.82	5.94
3.0	14.82	5.64
4.0	14.77	5.16
5.0	17.00	6.38
6.0	18.00	5.86
7.5	21.63	8.17
14.8	25.02	8.99
20.0	28.21	10.70

TABLE VIII

PROBABILITY/MeV FOR RADIATIVE-CAPTURE GAMMA RAYS FOR  $^{238}\text{U}$   
 (Normalized to One Photon per Capture)  
 $E_0 = 10^{-5}$  eV to 45 keV.

$\frac{E_0}{E_Y}$ (MeV)	6.7 eV	21.5 eV	37.1 eV	65.1 eV	80.9 eV	101.8 eV	118.2 eV	156.0 eV	198.9 eV	235.0 eV	273.2 eV	400.6 eV	750.8 eV	3.0 keV
0.0	0.0941	0.0873	0.105	0.120	0.117	0.147	0.133	0.124	0.139	0.189	0.185	0.176	0.130	0.170
0.1	0.113	0.103	0.118	0.141	0.137	0.168	0.153	0.142	0.159	0.210	0.208	0.195	0.147	0.196
0.2	0.134	0.120	0.135	0.166	0.162	0.192	0.176	0.162	0.188	0.232	0.229	0.215	0.162	0.222
0.3	0.161	0.142	0.152	0.198	0.196	0.219	0.202	0.180	0.213	0.260	0.259	0.238	0.179	0.262
0.4	0.188	0.166	0.169	0.230	0.227	0.245	0.231	0.214	0.242	0.291	0.283	0.263	0.195	0.299
0.5	0.216	0.192	0.189	0.270	0.265	0.272	0.260	0.249	0.272	0.323	0.313	0.284	0.214	0.348
0.6	0.251	0.220	0.209	0.312	0.303	0.297	0.292	0.279	0.303	0.321	0.346	0.308	0.237	0.395
0.7	0.284	0.252	0.236	0.352	0.352	0.327	0.327	0.321	0.335	0.383	0.372	0.330	0.262	0.446
0.8	0.318	0.285	0.256	0.390	0.395	0.356	0.359	0.356	0.366	0.415	0.403	0.356	0.288	0.500
0.9	0.351	0.322	0.283	0.444	0.441	0.384	0.385	0.410	0.398	0.447	0.432	0.382	0.317	0.562
1.0	0.378	0.362	0.310	0.428	0.474	0.410	0.407	0.480	0.429	0.462	0.449	0.406	0.353	0.604
1.25	0.444	0.455	0.381	0.439	0.451	0.470	0.449	0.609	0.486	0.439	0.406	0.458	0.464	0.488
1.50	0.491	0.621	0.554	0.463	0.500	0.495	0.550	0.569	0.556	0.466	0.497	0.546	0.565	0.513
1.75	0.530	0.581	0.615	0.471	0.512	0.438	0.449	0.510	0.461	0.324	0.464	0.424	0.477	0.427
2.00	0.487	0.495	0.511	0.380	0.416	0.406	0.401	0.465	0.433	0.360	0.406	0.488	0.470	0.333
2.25	0.378	0.405	0.378	0.313	0.331	0.308	0.320	0.256	0.294	0.406	0.337	0.305	0.301	0.210
2.50	0.237	0.193	0.260	0.253	0.198	0.249	0.247	0.141	0.161	0.204	0.132	0.156	0.249	0.106
2.75	0.135	0.116	0.165	0.133	0.104	0.146	0.108	0.0564	0.0994	0.103	0.0798	0.0778	0.134	0.0647
3.00	0.0815	0.0564	0.0956	0.0863	0.0605	0.0826	0.0897	0.0291	0.0657	0.0363	0.0602	0.0394	0.0883	0.0434
3.25	0.0497	0.0186	0.0453	0.0537	0.0384	0.0429	0.0429	0.0180	0.0298	0.0469	0.0199	0.0290	0.0497	0.0277
3.50	0.0162	0.0074	0.0211	0.0326	0.0373	0.0260	0.0226	0.0174	0.0145	0.0262	0.0290	0.0262	0.346	0.0137
3.75	0.0248	0.0279	0.0256	0.0140	0.0086	0.0156	0.0288	0.0180	0.0255	0.0204	0.0181	0.0272	0.0325	0.0081
4.00	0.0374	0.0286	0.0235	0.0175	0.0155	0.0044	0.0086	0.0082	0.0261	0.0385	0.0298	0.0519	0.0301	0.0161
4.25	0.0005	0.0022	0.0030	0.0082	0.0045	0.0078	0.0160	0.0134	0.0144	0.0094	0.0196	0.0143	0.0353	0.0050
4.50	0.0005	0.0018	0.0023	0.0044	0.0057	0.0066	0.0058	0.0089	0.0066	0.0045	0.0096	0.0073	0.100	0.0034
4.75	0.0009	0.0054	0.0012	0.0038	0.0048	0.0029	0.0048	0.0007	0.0098	0.0036	0.0030	0.0017	0.0030	0.0007
4.80	0.0001	0.0005	0.0	0.0002	0.0	0.0001	0.0002	0.0	0.0001	0.0002	0.0	0.0	0.0	0.0
4.90	0.0	0.0	0.0	0.0	0.0	0.0	0.0	0.0	0.0	0.0	0.0	0.0	0.0	0.0



TABLE IX  
 PROBABILITY/MeV FOR RADIATIVE-CAPTURE GAMMA RAYS FOR  $^{238}\text{U}$   
 (Normalized to One Photon per Capture)  
 $E_0 = 45 \text{ keV to } 1.09 \text{ MeV}$

$\frac{E_0}{E_\gamma}$ E <sub>γ</sub> (MeV)	45 keV	1.09 MeV
0.0	0.206	0.186
0.1	0.253	0.226
0.2	0.291	0.265
0.3	0.342	0.316
0.4	0.391	0.365
0.5	0.442	0.414
0.6	0.488	0.456
0.7	0.533	0.496
0.8	0.573	0.533
0.9	0.616	0.562
1.0	0.637	0.580
1.25	0.488	0.460
1.50	0.522	0.482
1.75	0.403	0.383
2.00	0.280	0.265
2.25	0.138	0.154
2.50	0.0558	0.0918
2.75	0.0316	0.0586
3.00	0.0195	0.0398
3.25	0.0082	0.0305
3.50	0.0108	0.0407
3.75	0.0043	0.0303
4.00	0.0039	0.0210
4.25	0.0028	0.0161
4.50	0.0017	0.0112
4.75	0.0005	0.0076
5.00	0.0	0.0052
5.25	0.0	0.0035
5.50	0.0	0.0023
5.75	0.0	0.0013
5.80	0.0	0.0011
5.85	0.0	0.0008
5.90	0.0	0.0001
6.00	0.0	0.0

TABLE X

## MULTIPLICITIES FOR GAMMA-RAY PRODUCTION FROM INELASTIC SCATTERING

 $E_0 = 45.189 \text{ keV to } 1.09 \text{ MeV}$ 

$E_Y$ (keV) $E_0$ (keV)	Total Multi- plicities	45	103	160	211	218	258	270	519
45.189	1.0000	1.0000							
148.622	1.0000	1.0000	0.0						
200.0	1.0434	1.0000	0.0434						
309.294	1.0880	1.0000	0.0880	0.0					
400.0	1.1402	1.0000	0.1229	0.0173					
521.180	1.2058	1.0000	0.1782	0.0276	0.0				
600.0	1.2803	1.0000	0.2223	0.0464	0.0116				
682.856	1.3524	1.0000	0.2632	0.0649	0.0243				
735.074	1.4090	0.9944	0.2927	0.0775	0.0337				
780.263	1.4719	0.9899	0.3194	0.0837	0.0376		0.0		
830.473	1.5681	0.9871	0.3749	0.0936	0.0485		0.0089		0.0
934.910	1.7297	0.9828	0.4358	0.1242	0.0717		0.0239		0.0048
953.990	1.9067	0.9735	0.4844	0.1651	0.0963	0.0	0.0370	0.0	0.0100
972.066	2.0338	0.9721	0.5141	0.1991	0.1165	0.0014	0.0455	0.0014	0.0139
997.171	2.1661	0.9692	0.5422	0.2339	0.1327	0.0027	0.0511	0.0027	0.0164
1039.347	2.2696	0.9663	0.5423	0.2756	0.1528	0.0036	0.0583	0.0045	0.0193
1064.452	2.3446	0.9594	0.5484	0.2970	0.1595	0.0053	0.0623	0.0057	0.0194
1090.0	2.4160	0.9476	0.5260	0.3121	0.1681	0.0074	0.0690	0.0079	0.0227
Excitation Energy (keV)	<u>All</u>	<u>45</u>	<u>148</u>	<u>308</u>	<u>519</u>	<u>950</u>	<u>777</u>	<u>950</u>	<u>827</u>
$E_Y$ (keV) $E_0$ (keV)	584	635	660	680	687	886	905	912	948
682.856		0.0		0.0					
735.074	0.0	0.0051		0.0056	0.0				
780.263	0.0102	0.0102		0.0102	0.0107				
830.473	0.0144	0.0129		0.0129	0.0149				
934.910	0.0215	0.0167		0.0268	0.0215	0.0			
953.990	0.0256	0.0218		0.0503	0.0285	0.0142	0.0		
972.066	0.0283	0.0237	0.0	0.0534	0.0292	0.0329	0.0023		
997.171	0.0292	0.0319	0.0064	0.0638	0.0333	0.0451	0.0055		0.0
1039.347	0.0332	0.0305	0.0139	0.0672	0.0354	0.0542	0.0081		0.0022
1064.452	0.0336	0.0309	0.0208	0.0760	0.0380	0.0641	0.0110	0.0	0.0044
1090.0	0.0384	0.0345	0.0262	0.0781	0.0397	0.0760	0.0131	0.0074	0.0087
Excitation Energy (keV)	<u>732</u>	<u>680</u>	<u>968</u>	<u>680</u>	<u>732</u>	<u>931</u>	<u>950</u>	<u>1060</u>	<u>993</u>
$E_Y$ (keV) $E_0$ (keV)	990	1015	1035						
997.171	0.0								
1039.347	0.0022								
1064.452	0.0066	0.0	0.0022						
1090.0	0.0179	0.0087	0.0065						
Excitation Energy (keV)	<u>993</u>	<u>1060</u>	<u>1035</u>						

TABLE XI  
 GAMMA-RAY MULTIPLICITIES FOR  $^{238}\text{U}$   
 $E_0 = 10^{-5}$  eV to 1.09 MeV

$E_0$	Fission	Radiative Capture	Inelastic
$10^{-5}$ eV	--	2.98	--
6.7 eV	--	2.98	--
21.5 eV	--	3.01	--
37.1 eV	--	2.88	--
65.1 eV	--	3.09	--
80.9 eV	--	3.17	--
101.8 eV	--	3.14	--
118.2 eV	--	3.09	--
156.0 eV	--	3.32	--
198.9 eV	--	3.17	--
235.0 eV	--	3.26	--
273.2 eV	--	3.29	--
400.6 eV	--	3.24	--
750.8 eV	--	2.92	--
3.0 keV	--	3.06	--
45.189 keV	--	3.95	1.0000
200.0 keV	--	4.18	1.0434
400.0 keV	--	4.25	1.1402
600.0 keV	--	4.32	1.2803
735.074 keV	7.174	4.36	1.4090
830.473 keV	7.174	4.39	1.5681
934.910 keV	7.174	4.43	1.7297
953.990 keV	7.174	4.43	1.9067
997.171 keV	7.174	4.45	2.1661
1064.452 keV	7.174	4.47	2.3446
1090.0 keV <sup>a</sup>	7.174	4.48	2.4160

<sup>a</sup> For  $E_0 > 1.09$  MeV, use the gamma-ray production cross sections in barns/MeV provided in Table XII.

TABLE XII  
 GAMMA-RAY PRODUCTION CROSS SECTIONS FOR  $^{238}\text{U}$ , IN BARNS/MeV

$E_0$ (MeV) $E_\gamma$ (MeV)	1.09	2.0	3.0	4.0	5.0	14.8	20.0
0.0	1.09	5.49	5.88	7.02	8.54	10.19	10.53
0.1	4.93	6.47	7.06	8.84	10.65	12.43	12.37
0.2	8.04	7.50	8.01	9.99	12.21	14.16	14.35
0.3	8.30	8.58	8.91	11.24	13.68	15.59	16.37
0.4	6.22	9.23	9.39	11.72	14.51	16.20	17.95
0.5	4.49	9.18	9.36	11.53	14.51	15.69	18.02
0.6	3.00	8.79	8.90	9.90	12.95	14.06	17.53
0.7	1.85	7.76	7.54	7.98	10.47	11.51	16.11
0.8	1.17	6.73	5.88	6.34	8.13	9.24	13.22
0.9	0.770	5.68	4.65	5.22	6.27	7.54	9.82
1.0	0.493	4.79	3.77	4.56	5.22	6.19	7.85
1.25	0.245	3.09	2.86	3.38	3.63	4.36	5.05
1.50	0.213	2.04	2.44	2.76	2.84	3.44	3.89
1.75	0.192	1.27	1.99	2.23	2.30	2.63	2.62
2.00	0.171	0.740	1.53	1.82	1.88	1.95	1.75
2.25	0.133	0.440	1.12	1.38	1.45	1.42	1.16
2.50	0.0937	0.294	0.749	1.01	1.10	1.04	0.833
2.75	0.0622	0.209	0.493	0.663	0.780	0.756	0.653
3.00	0.0424	0.154	0.334	0.416	0.551	0.547	0.523
3.25	0.0296	0.113	0.229	0.292	0.384	0.379	0.417
3.50	0.0206	0.087	0.164	0.216	0.284	0.282	0.322
3.75	0.0140	0.067	0.117	0.160	0.212	0.215	0.244
4.00	0.0098	0.052	0.085	0.123	0.163	0.167	0.182
4.25	0.0066	0.040	0.063	0.092	0.122	0.131	0.138
4.50	0.0045	0.032	0.046	0.071	0.095	0.105	0.104
4.75	0.0032	0.025	0.033	0.054	0.073	0.084	0.079
5.00	0.0022	0.020	0.025	0.042	0.056	0.067	0.058
5.5	0.0017	0.012	0.014	0.025	0.033	0.044	0.032
6.0	0.0005	0.007	0.008	0.015	0.020	0.029	0.018
6.5	0.0003	0.0	0.002	0.009	0.012	0.019	0.0098
7.0	0.0001	0.0	0.0	0.002	0.007	0.013	0.006
8.0	0.0	0.0	0.0	0.0	0.0	0.0	0.0

TABLE XIII  
 TOTAL GAMMA-RAY PRODUCTION CROSS SECTIONS FOR  $^{238}\text{U}$

$E_0$ (MeV)	$\int_0^{8.0 \text{ MeV}} \sigma_{\text{prod}}(E_\gamma) dE_\gamma$ (barns)	$\int_0^{0.5 \text{ MeV}} \sigma_{\text{prod}}(E_\gamma) dE_\gamma$ (barns)
1.09	4.32	3.03
2.1	10.24	3.92
3.0	10.99	4.11
4.0	13.11	5.12
5.0	15.66	6.26
14.8	17.65	7.14
20.0	20.03	8.25